DOI: 10.1002/ ((please add manuscript number))
Article type: Full Paper

Codelivery of NOD2 and TLR9 Ligands via Nanoengineered Protein Antigen Particles for Improving and Tuning Immune Responses

*Katelyn T. Gause, Yan Yan, Neil M. O'Brien-Simpson, Jiwei Cui, Jason C. Lenzo, Eric C. Reynolds, Frank Caruso**

Dr. K. T. Gause, Dr. Y. Yan, Dr. J. Cui, Prof. F. Caruso
ARC Centre of Excellence in Convergent Bio-Nano Science and Technology, and the Department of Chemical and Biomolecular Engineering, The University of Melbourne, Parkville, Victoria 3010, Australia
E-mail: fcaruso@unimelb.edu.au
A/Prof. N. M. O'Brien-Simpson, Dr. J. C. Lenzo, Prof. E. C. Reynolds
Melbourne Dental School, Oral Health CRC, The University of Melbourne, Parkville, Victoria 3010, Australia
Dr. Y. Yan
Present address: Centre for BioNano Interactions, University College Dublin, Dublin 4, Ireland

Keywords: adjuvant, vaccine, protein particles, codelivery, mesoporous silica

ABSTRACT

Vaccine adjuvants that can induce robust protective immunity are highly sought after for the development of safer and more effective vaccines. Vaccine formulation parameters that govern efficacy are still far from clear, such as the diverse impacts of codelivering agonist molecules for innate cell receptors (i.e., pattern recognition receptors, PRRs). In this study, a mesoporous silica (MS)-templating approach is used to fabricate protein antigen (ovalbumin) particles covalently functionalized with agonists for NOD-like receptor 2 (NOD2) and Toll-like receptor 9 (TLR9). Particle-induced combinatorial NOD2/TLR9 signaling results in synergistic inflammatory cytokine secretion by mouse macrophages (RAW 264.7). Administration of NOD2/TLR9 particles in mice results in adaptive immune responses that are both quantitatively and qualitatively different than those resulting from administration of particles conjugated with either NOD2 or TLR9 agonists alone. While delivery of NOD2 agonists alone activates T helper 2 (Th2)-type responses (no CD8+ T cell activation) and delivery of TLR9 agonists alone activates CD8+ T cell and T helper 1 (Th1)-type responses, codelivery of NOD2 and TLR9 agonists enhances Th1-type responses and abrogates CD8+ T cell activation. The results illustrate that in the particle-based system, NOD2 activation plays different roles in polarizing adaptive immune responses depending on coactivation of TLR9.

1. Introduction

Most vaccine formulations require adjuvants to induce immune responses that are sufficient to result in protective immunity. Aluminum salt- and emulsion-based adjuvants used in currently licensed vaccine formulations induce primarily humoral immune responses characterized by antibody production and T helper 2 (Th2) cells, which predominantly produce the cytokine interleukin (IL)-4.[1] However, these types of responses are not sufficient for protection against many chronic infections (e.g., HIV) and cancers, which require robust cell-mediated responses carried out by T helper 1 (Th1) and CD8+ T cells, which predominantly produce the cytokine interferon (IFN)-γ.[2] The quantity and quality of T cell activation relies on recognition by innate immune cells via pattern recognition receptors (PRRs). The agonists of many PRRs have been identified and recent studies have shown that PRRs can be activated to induce specific types of immune responses that can be synergistically enhanced through coactivation of various PRR combinations.[3,4]

Two of the most widely studied classes of PRRs are toll-like receptors (TLRs) and NOD-like receptors (NLRs), which are transmembrane and cytosolic receptors, respectively. TLRs are localized on the surface and/or endosomal membranes of innate immune cells and recognize microbial patterns that are common to both commensal and pathogenic microbes. Cytosolic PRRs (e.g., NODs) can detect signals deriving from intracellular infection, which may be an important aspect of the immune system's ability to distinguish between commensal and pathogenic organisms.[5] Of the known PRR ligands, TLR ligands have been the most extensively studied for use in adjuvant formulations, with many in clinical trials and one on the market.[6] The more recently discovered NOD agonists are also currently under investigation for use as adjuvants.[7] Administration of endosomal TLR agonists typically polarizes Th1[4,8] and CD8+ T cell[9,10] responses while NOD agonists polarize primarily Th2 responses.[11] However, recent studies have shown that NOD signaling is crucial for optimal

induction of both Th1 and Th2 immune responses upon administration of Complete Freund's Adjuvant (CFA), which contains both TLR and NOD agonists;[11] suggesting that NOD signaling plays different roles in shaping adaptive immunity depending on coactivation of TLRs. Several recent studies have shown that simultaneous stimulation of NODs and TLRs synergistically enhances innate inflammatory immune responses, confirming the existence of crosstalk between TLRs and NODs, which may be beneficial for use in vaccine adjuvants.[3,12,13]

Recently, Pavot et al. reported an investigation of a NOD/TLR adjuvant system using a chimeric ligand containing a TLR2 and NOD2 agonist.[13] The chimeric ligand synergistically enhanced innate immune responses in both human and mouse dendritic cells (DCs) in vitro and Th1-polarized serum antibody production following subcutaneous administration. However, responses induced by single agonists were not strong enough to elucidate the potentially complex roles of NOD signaling. Systems that enable the delineation of single and combinatorial PRR signaling are required to fully understand the downstream immune responses induced by PRR-targeted adjuvants.[4]

Soluble vaccine components are typically not sufficiently immunogenic to result in protective immunity. This is primarily because diffusion and clearance of soluble material inhibits the required local concentration of antigen necessary for inducing immune responses. Particulate systems are inherently more immunogenic than soluble systems, thus soluble vaccine components can be formulated into particulate systems to improve immune responses.[14] Additionally, current fabrication techniques allow nanoscale control and characterization of physicochemical properties, which can significantly affect interactions with the immune system. Particle templating approaches can be exploited for such applications, as they result in high particle uniformity and monodispersity. Porous particles are especially advantageous for their characteristically high surface areas compared with solid particles,

which facilitates adsorption of a relatively higher amount of cargo (e.g., antigen, PRR agonist molecules). Mesoporous silica (MS)-mediated polymer particles with tunable size, elasticity, and surface chemistry meet the requirements for these applications.[15] Our previous study showed that ovalbumin (OVA) particles fabricated via MS templating and amide bond crosslinking induced significantly better antigen-specific immune responses in mice compared with soluble OVA.[16] We showed that particles fabricated with reduced OVA induced significantly increased antigen-specific immune responses compared with native analogs, whereas oxidization of OVA resulted in a significant decrease in antigen-specific immune responses.

In this study, NOD2 and TLR9 agonists (muramyl dipeptide (MDP) and CpG oligonucleotides (ODNs), respectively) were chemically conjugated to reduced OVA particles engineered via MS templating. All experimental groups were conjugated with either a positive or negative analog of each agonist, where corresponding analogs share a similar structure and chemical reactivity. Thus, experimental groups maintain consistent physicochemical properties and the roles of NOD2, TLR9, and NOD2/TLR9 combinatorial signaling could be delineated. The results showed that particles containing MDP and CpG had a synergistic effect on cytokine secretion by a mouse macrophage cell line (i.e., RAW 264.7, RAW) compared with particles containing only one PRR agonist, confirming synergistic crosstalk between NOD2 and TLR9 induced by the particle system. Following administration in mice, MDP particles induced Th2-polarized CD4+ T cell and antibody responses and no CD8+ T cell responses, whereas CpG particles induced Th1-polarized CD4+ T cell and antibody responses and significant CD8+ T cell responses. Immunization with MDP/CpG particles showed significantly enhanced Th1-polarized CD4+ T cell and antibody responses compared with MDP and CpG particles. Compared with CpG particles, however, there was a decrease in CD8+ T cell responses. The results indicate that while NOD2 and TLR9 co-activation

induced by the particles results in synergistic innate and adaptive immune responses, NOD2 activation plays different roles in polarizing adaptive immune responses depending on coactivation of TLR9. The results indicate that codelivery of different combinations of PRR ligands via particle-based systems may enable tunability of protective immunity by enhancing and suppressing specific types of immune responses activated during immunization.

2. Results and Discussion

In our previous study, we used a MS particle templating approach to show that the reduction of OVA significantly enhanced antigen-specific immune responses compared with native and oxidized analogs.[16] Therefore, reduced OVA particles (abbreviated as OVA particles) fabricated via MS particle templating were rationally selected for functionalization with NOD2 and TLR9 agonists (i.e., MDP and CpG ODNs, respectively). MDP is the minimal bioactive peptidoglycan (PGN) motif common to all bacteria (Scheme S1a). The adjuvant activity of MDP is highly stereospecific, where the L-D isomer is recognized and not the D-D or L-L analogs.[17] Therefore, a stereoisomer of the L-D isomer was used as the negative control (Scheme S1b). Notably, MDP has also been implicated in the activation of the NALP3 inflammasome.[18] TLR9 is an endosomal membrane PRR that recognizes single stranded, unmethylated CpG motifs that are common in viral DNA. In this study, a class B CpG ODN specific for murine TLR9 was selected with a sequence of 5'- TCC ATG ACG TTC CTG ACG TT -3' and a nuclease-resistant phosphorothioate backbone. ODN analogs containing GpC dinucleotides instead of CpG dinucleotides were used as the negative control. Particles were fabricated to contain the four possible combinations using MDP (M+), MDP negative control (M-), CpG ODN (C+), and GpC ODN negative control (C-). In the following sections, particles are referred to as M-C-, M+C-, M-C+, and M+C+ to describe their conjugated

ligands. Some experiments also include an additional "naked" group that refers to particles used in our previous study[16] that do not contain conjugated ligands.

2.1. Particle Preparation

The four types of particles used in this study (M-C-, M+C-, M-C+, M+C+) were fabricated according to **Scheme 1**. First, OVA was loaded via electrostatic interactions into amine-functionalized MS templates with an average diameter of 1 μm and bimodal pore sizes of approximately 2-3 nm and 10-40 nm (Figure S1a,b), OVA-loaded MS particles were then treated with a reducing agent, dithiothreitol (DTT), according to our previous study.[16] MDP was covalently conjugated to primary amines present in OVA via amide formation. This was achieved by adding excess MDP to the particle mixture in the presence of 4-(4,6-dimethothy-1,3,5-triazin-2-yl)-4-methylmorpholinium chloride (DMTMM), which is a coupling reagent that activates carboxylic acid groups in MDP to form amide bonds with primary amines in OVA. Notably, DMTMM used in this step also stabilized the particles via amide bond formation in OVA. Following treatment with DMTMM, particles were washed and then treated with 5,5'-dithiobis-(2-nitrobenzoic acid) (DTNB) at pH 8, which reacts with free thiols in OVA resulting in the stoichiometric formation of disulfide bonds in OVA and release of TNB^{2-} ions. The concentration of TNB^{2-} ions can be measured by the absorbance of the supernatant at 412 nm to quantify the reaction between DTNB and free thiols in the OVA. Particles were then extensively washed to remove TNB^{2-} ions and excess DTNB, ensuring that the disulfides in the OVA were the only thiol reactive species present. Next, CpG ODNs with a thiol attached to the 3' flanking region (referred to as CpG) were added to the system at pH 7.2, which underwent a thiol/disulfide exchange reaction with the disulfide bonds in the OVA. CpG conjugation releases TNB^{2-} ions into the supernatant also at a 1:1 stoichiometric ratio. Therefore, the moles of TNB^{2-} ions in the supernatant are equivalent to the moles of CpG conjugated to the particles. Using the Beer-Lambert Law and extinction coefficient of

TNB^{2-} at 412 nm (14,150 M^{-1} cm^{-1}), the amount of CpG conjugated was calculated to be 2.6 (± 0.2) × 10^{-20} moles per particle. In addition, the concentration of single-stranded DNA (ssDNA) can be quantified using the measured absorbance at 260 nm, Beer-Lambert Law, and extinction coefficient of ssDNA (0.027 $(\mu g/mL)^{-1}$ cm^{-1}). Using this technique, the conjugated CpG was found to be 3.4 (± 0.8) × 10^{-20} moles per particle, which is in good agreement with the value calculated from the TNB^{2-} concentration. CpG conjugated with FITC at the 5' flanking region was used in the procedure described above and the attachment of CpG was confirmed by visualization of the FITC fluorophore using fluorescence microscopy (Figure S2). As a result of amide bond formation with DMTMM, stable, freestanding particles were obtained after template removal with HF/NH_4 buffer (pH ~5) (Figure S1c). Notably, freestanding particles were not obtained without amide bond formation via treatment with DMTMM.

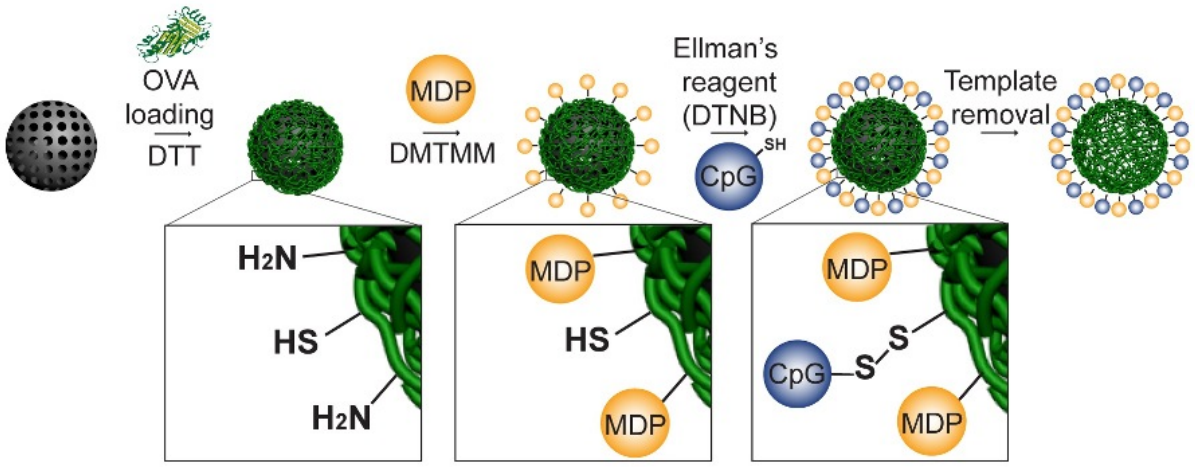

Scheme 1. Schematic representation of the fabrication of OVA particles with functionalization with MDP and CpG. OVA is loaded into amine-modified MS particles (diameter ~1 μm) via electrostatic interactions and then reduced with DTT. Loaded OVA is then treated with MDP and DMTMM to both conjugate MDP to amines in OVA and crosslink OVA via amide bonds. DTNB is then added to form a mixed disulfide with the free thiols in OVA, releasing TNB^{2-} ions in a 1:1 stoichiometric ratio. CpG with a thiol conjugated

at the 3' flanking region undergoes a thiol/disulfide exchange with the mixed disulfide, releasing a TNB^{2-} ion in a 1:1 stoichiometric ratio. Finally, MS templates are removed via dissolution with HF/NH_4 buffer (pH ~5).

2.2. NOD2 and TLR9 Activation by Particles

Specific activation of NOD2 and TLR9 by the particles was determined using HEK298 reporter cell lines for NOD2 and TLR9 stimulation (i.e., HEK-mNOD2 and HEK-mTLR9, respectively). HEK293 reporter cell lines are stably transfected to express a secreted embryonic alkaline phosphatase (SEAP) gene that is inducible by PRR activation. HEK-mNOD2 and HEK-mTLR9 express high levels of murine NOD2 and TLR9 on the cell surface as well as endogenous levels of TLR3, TLR5, and NOD1. Therefore, parental cell lines (i.e., HEK-Null1, HEK-Null2) that also express the SEAP reporter gene, but are not transfected with NOD2 or TLR9 genes were used as negative controls to verify NOD2 and TLR9-specific responses. Cells were incubated with particles (100:1 particle-to-cell ratio, 24 h) and the SEAP in the supernatant was measured using QUANTI-Blue. Results showed that M+C- and M+C+ particles activated HEK-mNOD2 cells while M-C+, M-C-, and naked particles did not activate the cells above the background (blank) control **(Figure 1a)**. Similarly, M-C+ and M+C+ particles activated HEK-mTLR9 cells, whereas M+C-, M-C-, and naked particles did not (Figure 1b). No significant activation of either the HEK-Null2 or HEK-Null1 cells was observed (Figure 1, white bars), indicating that the particles specifically activated NOD2 or TLR9 and no other HEK endogenous receptors that could induce NF-κB.

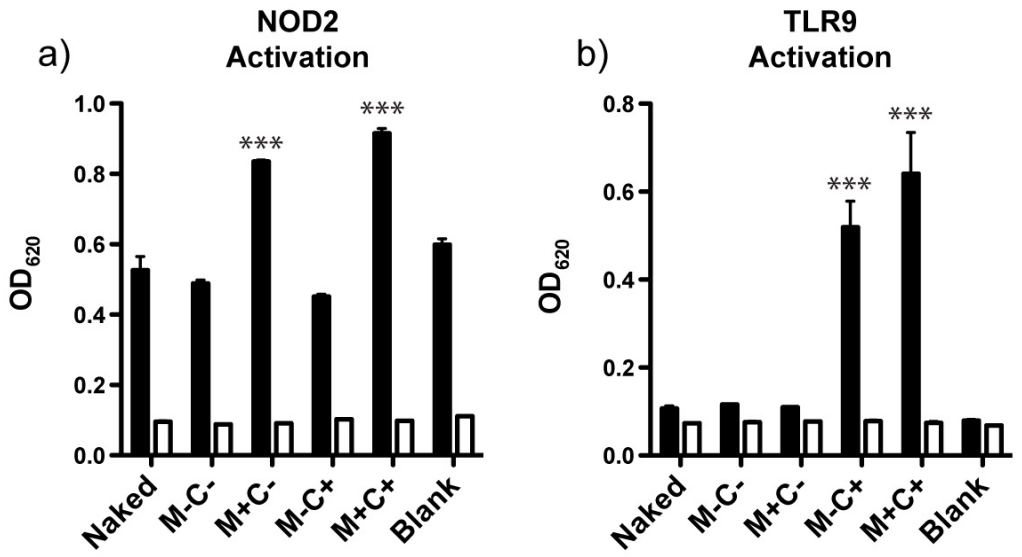

Figure 1. NF-κB activation in NOD2- (a) and TLR9- (b) expressing HEK293 reporter cell lines measured by optical density at 620 nm of SEAP secretion. Activation of HEK-mNOD2 (a) and HEK-mTLR9 (b) cells are shown as black bars and respective parental cell lines (i.e., HEK-Null1, HEK-Null2) are shown as white bars. Cells were incubated with particles at a particle-to-cell ratio of 100:1 for 24 h at 37 °C, 5% CO_2. Data are expressed as mean ± standard deviation; *$p < 0.05$, **$p < 0.01$, ***$p < 0.001$ (one-way ANOVA, Bonferroni multiple comparisons test). Data are representative of five independent experiments.

2.3. Inflammatory Responses in Mouse Macrophages

NF-κB activation is implicated in both TLR and NOD signaling pathways. Particle-induced activation of NF-κB in mouse macrophages was determined using the RAW-Blue reporter cell line, which expresses both TLR9 and NOD2 in their native locations (i.e., endosome and cytoplasm, respectively). This technique is commonly used to measure PRR-associated inflammatory responses induced by other systems, including particulate systems carrying PRR agonists.[19] Cells were incubated with particles (100:1 particle-to-cell ratio, 24 h) and the SEAP in the supernatant was measured using QUANTI-Blue **(Figure 2)**. Both M+C- and M-C+ particles induced activation that was significantly higher than M-C- and naked particles

($p < 0.001$) and M+C+ particles induced activation significantly higher than both M+C- and M-C+ particles ($p < 0.001$). Thus, simultaneous stimulation of NOD2 and TLR9 in the same cell increased activation of NF-κB, indicating that the intracellular pathways activated by these receptors do not inhibit each other. Our data corroborates a similar finding where a TLR2/NOD2 chimeric ligand induced an additive activation effect in macrophages compared with single NOD2 and TLR2 ligands.[13] Pro-inflammatory responses induced by MDP[19,20] or CpG ODN[21] delivered individually in particle-based systems have also been observed in other studies (i.e., not combined such as in the current study). Taken together, the results confirm that the OVA particles are an effective delivery system for NOD2 and TLR9 agonists and codelivery enhances NF-κB activation in macrophages.

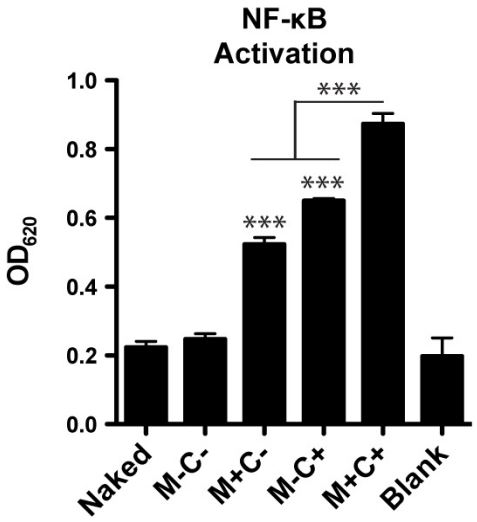

Figure 2. NF-κB transcription factor activation in macrophages (RAW-Blue cells) measured by optical density at 620 nm of SEAP secretion. Cells were incubated with particles at a particle-to-cell ratio of 100:1 for 24 h at 37 °C, 5% CO_2. Data are expressed as mean ± standard deviation; *$p < 0.05$, **$p < 0.01$, ***$p < 0.001$ (one-way ANOVA, Bonferroni multiple comparisons test). Data are representative of five independent experiments.

The concentrations of various cytokines secreted by macrophage (RAW) cells incubated with particles (100:1 particle-to-cell ratio, 24 h) were measured using a Bio-Plex assay

(Figure 3). M+C- and M-C+ particles induced significantly more TNF-α secretion than M-C- and naked particles ($p < 0.001$); and M+C+ particles induced significantly more TNF-α secretion than M+C- and M-C+ particles ($p < 0.001$). Thus, costimulation of NOD2 and TLR9 enhanced TNF-α secretion, but not synergistically. However, costimulation did synergize the secretion of IL-1β, IL-10, and GM-CSF. This is in agreement with other studies that have demonstrated enhanced and synergistic cytokine secretion induced by TLR and NOD receptors.[3,12,13] The specific molecular mechanism responsible for the synergistic effect of NOD agonists on TLR-mediated cytokine production is unclear.[22,23] However, it has been shown that NOD2 stimulation upregulates MyD88 expression.[24] TAK1, a molecule involved in MyD88-dependent TLR signaling has also been shown to participate in the NOD2 pathway,[25] which may be implicated in the observed synergy. It is also possible that a variety of different mechanisms contribute to NOD/TLR synergy and that not a single mechanism is responsible for the overall effect.[22]

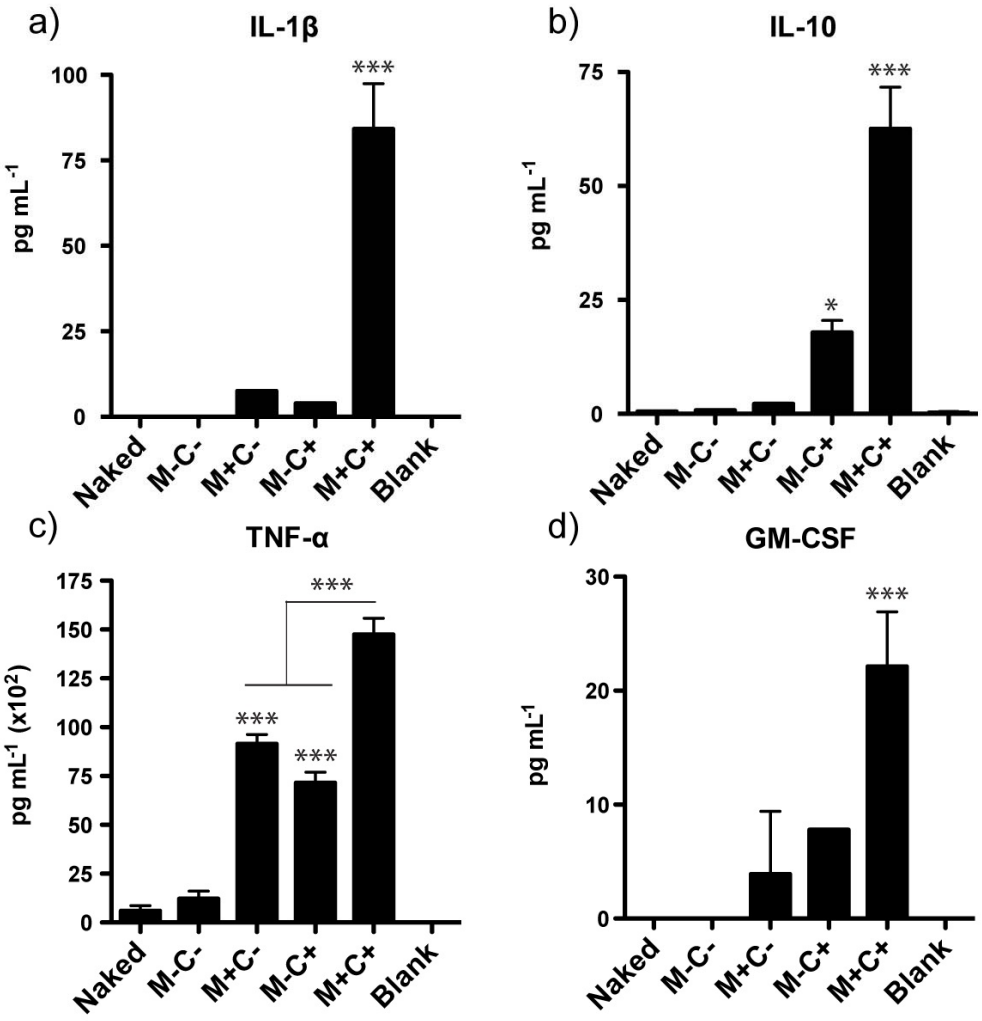

Figure 3. Concentration of IL-1β (a), IL-10 (b), TNF-α (c), and GM-CSF (d) secretion by macrophage (RAW) cells measured with a Bio-Plex assay. Cells were incubated with particles at a particle-to-cell ratio of 100:1 for 24 h at 37 °C, 5% CO_2. Data are expressed as the mean ± standard deviation; *$p < 0.05$, **$p < 0.01$, ***$p < 0.001$ (one-way ANOVA, Bonferroni multiple comparisons test). Data are representative of two independent experiments.

One interesting aspect of the data shown in Figure 3 is the synergistic secretion of IL-1β. The secretion of IL-1β is a cytokine associated with activation of the caspase-1 inflammasome, which processes intracellular pro IL-1β and IL-18 into their bioactive forms. RAW cells, however, do not express the ASC adaptor molecule necessary for activating caspase-1, and therefore cannot produce bioactive IL-1β or IL-18.[26] Typically in the absence

of caspase-1 activation, very little pro IL-1β and IL-18 is secreted and most is degraded within the cell.[27] Pelegrin et al., however, showed that stimulation with LPS (TLR4 agonist) and ATP (NLRP3 agonist) induced secretion of the pro-IL-1β precursor by RAW cells,[26] suggesting that NLRP3 activation can facilitate the release of the pro IL-1β from RAW cells through a caspase-1-independent mechanism. It is likely that a similar mechanism occurred in the current experimental setup. However, MDP also activates NLRP3,[18] and so it is unknown whether the current results reflect NOD2- or NLRP3- mediated release of the pro IL-1β.

2.4. CD4+ T cell Activation In Vivo

To measure adaptive immune responses induced by the particles in vivo, mice were immunized with particles intraperitoneally (day 0) and then subcutaneously (day 21). Three weeks (day 42) after the secondary immunization, CD4+ T cells were isolated from spleens and proliferation in response to OVA protein was determined, as we described previously **(Figure 4a)**.[16] Values for each group were normalized by dividing the cell count measured in response to OVA protein by the cell count measured in the absence of OVA protein. CD4+ T cells from mice immunized with M+C- or M-C+ particles showed similar levels of proliferation compared with those from M-C- immunized mice. However, M+C+ CD4+ T cells had a significantly higher ($p < 0.01$) proliferative response than CD4+ T cells from all other particle-immunized groups. Further, M+C+ CD4+ T cells proliferated to the same extent as those from mice immunized with an oil-in-water emulsion of OVA protein and Incomplete Freund's Adjuvant (IFA) (OVA/IFA, positive control). This indicates that codelivery of NOD2 and TLR9 agonists in vivo significantly enhances OVA-specific CD4+ T cell responses in the spleens of immunized mice.

The effector functions of OVA-specific CD4+ T cells (i.e., Th1 versus Th2) were determined using an ELISPOT assay, which measures the number of activated CD4+ T cells

producing either IL-4 or IFN-γ (characteristic of Th2 and Th1 CD4+ T cells, respectively) upon stimulation with OVA protein ex vivo (Figure 4b,c). Stimulation with OVA protein induced significant ($p < 0.01$) levels IL-4-secreting CD4+ T cells in the M+C- group, which was not observed in M-C+ and M+C+ groups (Figure 4b, black versus white bars). A significant number of M-C+ ($p < 0.01$) and M+C+ ($p < 0.001$) CD4+ T cells secreted IFN-γ upon restimulation, whereas M+C- CD4+ T cells did not show significant secretion of IFN-γ (Figure 4c, black versus white bars). Notably, there was no significant production of IL-17A by CD4+ T cells, as measured by the ELISPOT assay (Figure S3). The concentration of Th1 and Th2 characteristic cytokines were also measured using a Bio-Plex assay. Consistent with ELISPOT results, M+C- CD4+ T cells secreted significantly more IL-4 and IL-5 than M-C- and M-C+ CD4+ T cells ($p < 0.001$) (Figure 4d,e). Although M+C+ CD4+ T cells secreted significantly more IL-4 than M-C- CD4+ T cells ($p < 0.01$), the concentration was significantly lower than observed in the M+C- group ($p < 0.001$). IL-5 secretion by M-C+ and M+C+ CD4+ T cells was significantly lower than M-C- CD4+ T cells ($p < 0.01$). Additionally, M-C+ and M+C+ CD4+ T cells secreted significantly higher levels of IFN-γ than M-C- and M+C- CD4+ T cells ($p < 0.001$). M+C+ CD4+ T cells secreted significantly (3-fold) more IFN-γ than M-C+ CD4+ T cells. Taken together, the results demonstrate that NOD2 and TLR9 signaling induced by the particle system led to Th2- and Th1-polarized CD4+ T cell responses, respectively. Costimulation of both NOD2 and TLR9 was found to synergistically enhance Th1 and inhibit Th2 responses. Thus, NOD2 signaling plays different roles in activating adaptive responses depending on costimulation by TLR9. These results are in good agreement with other studies that have shown NOD signaling in the absence of TLRs induces Th2-polarized responses; and that NOD signaling facilitates TLR-driven Th1 responses.[11]

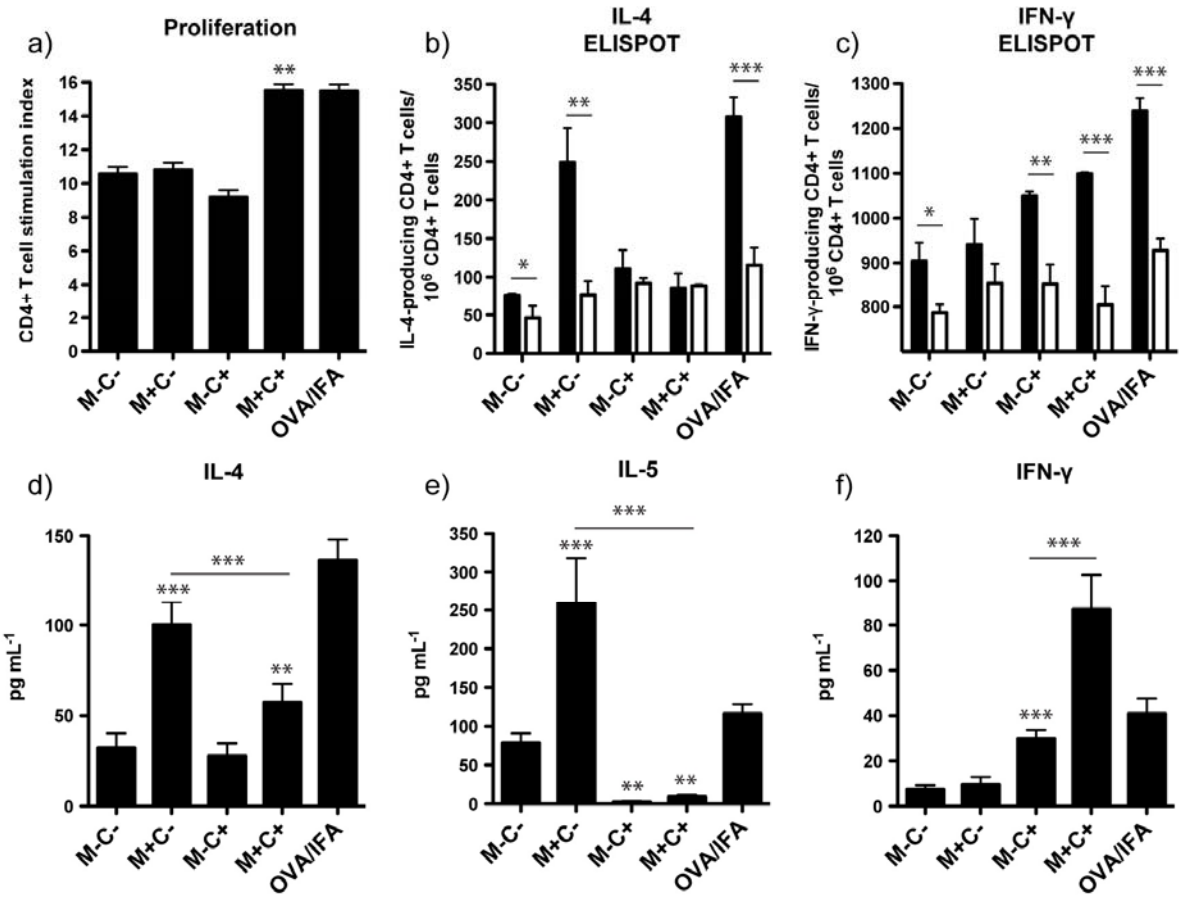

Figure 4. CD4+ T cell activation in vivo: a) Proliferation in the presence of naïve splenocyte APCs and 10 μg mL^{-1} OVA protein at 37 °C, 5% CO_2 ex vivo for 4 days measured by the cellular incorporation of 3H-thymidine. The number of IL-4- (b) and IFN-γ- (c) producing CD4+ T cells per million CD4+ T cells when stimulated with splenocyte APCs and 2.5 μg OVA protein at 37 °C, 5% CO_2 ex vivo for 3 days measured using an ELISPOT assay (white bars represent samples in the absence of OVA protein). The concentration of IL-4 (d), IL-5 (e), and IFN-γ (f) secreted by CD4+ T cells when stimulated with splenocyte APCs and 10 μg OVA at 37 °C, 5% CO_2 ex vivo for 3 days measured using a Bio-Plex assay. Data are expressed as mean ± standard deviation; *$p < 0.05$, **$p < 0.01$, ***$p < 0.001$; a, d-f: one-way ANOVA, Bonferroni multiple comparisons test; b-c: *t*-test. Each group shows data obtained from pooled cells of five individual mice.

2.5. Serum Antibody Production

In mice, a predominant production of sera IgG1 is often associated with Th2-polarized adaptive immune responses, while Th1-mediated responses are associated with predominantly IgG2 and IgG3 production. Mice were bled three weeks after the secondary immunization and the OVA-specific total IgG, IgG1, IgG2a, IgG2b, and IgG3 levels in the sera were measured by ELISA **(Figure 5)**. Notably, none of the particles induced significant IgG2a or IgG3 production. M+C-, M-C+, and M+C+ particles induced significantly more IgG production than M-C- and naked particles ($p < 0.001$), but there were no significant differences in the total IgG titer across these three groups (Figure 5a). Only M+C- ($p < 0.01$) and M+C+ ($p < 0.05$) particles induced significant IgG1 production compared with M-C- and naked particles (Figure 5b), which is consistent with Th2-polarization observed in CD4+ T cell responses (Figure 4b,d,e). M-C+ and M+C+ induced significant IgG2b production compared with M-C- and naked particles ($p < 0.001$). Additionally, M+C+ particles induced significantly more IgG2b production than M-C+ particles ($p < 0.05$). These results are also consistent with Th1-polarization observed in M+C- CD4+ T cells, which was enhanced in M+C+ CD4+ T cells (Figure 4c,f). Given the agreement between the polarization of CD4+ T cell responses and antibody production, it is likely that B cell activation was largely facilitated by activated CD4+ T cells. However, B cells can also be activated by direct engagement of PRRs.[28,29] It has been shown that CpG can act directly on B cells to enhance IgG2 responses and suppress IgG1[30] and that NOD activation can enhance TLR-driven proliferation of B cells.[29] Therefore, antibody production may also reflect intrinsic PRR signaling in B cells. Pavot et al. showed that a NOD2/TLR2 chimeric ligand could synergistically enhance the total sera IgG, IgG1, IgG2a, and IgA with polarization towards Th1-characteristic IgG2a.[13] Our data also show that coactivation of TLR9 and NOD2 enhances Th1-characteristic antibody responses (i.e., IgG2b). This data, in addition to the data in Figure 4, clearly indicates a different role of

NOD2 signaling in polarizing CD4+ T cell and antibody responses that depends on coactivation by TLR9.

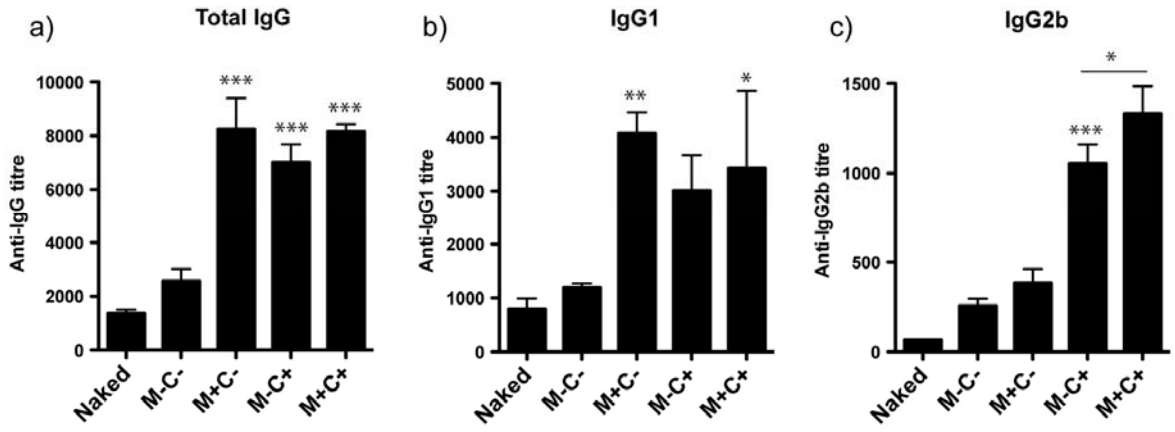

Figure 5. Serum OVA-specific IgG (a), IgG1 (b), and IgG2b (c) titers measured using an ELISA assay. Data are expressed as mean ± standard deviation; *p < 0.05, **p < 0.01, ***p < 0.001 (one-way ANOVA, Bonferroni multiple comparisons test). Each group shows data obtained from 5 individual mice. Data are representative of two independent experiments.

2.6. CD8+ T cell and CTL Activation In Vivo

The ability of PRR and OVA loaded particles to induce an OVA-specific CD8+ T cell response in vivo was measured using a variety of assays. CD8+ T cells were isolated from spleens of immunized mice and the OVA-specific IFN-γ response was determined by ELISPOT. CD8+ T cells from M-C+ ($p < 0.01$) and M+C+ ($p < 0.05$) groups were significantly restimulated by OVA protein ex vivo (**Figure 6a**, black versus white bars). Notably, the number of IFN-γ- secreting CD8+ T cells was more significant in the M-C+ group than in the M+C+ group ($p < 0.01$ versus $p < 0.05$). Thus, the results may indicate that NOD2 signaling inhibits CD8+ T cell responses. Using a fluorescent tetramer of MHC class I molecules loaded with OVA epitopes (SIINFEKL), the number of OVA-specific CD8+ T cells in the total CD8+ T cell population of each immunized group was quantified (Figure 6b). The M-C+ particle-immunized group had a significantly higher number of OVA-specific

CD8+ T cells compared with all other particle-immunized groups, which all had similarly low numbers of OVA-specific CD8+ T cells. The ability of each particle to prime an in vivo CTL response was determined by administering a mixture of target and control splenocytes 6 days after the booster immunization via intravenous tail vein injection. The OVA-specific cell lysis (i.e., the change in the proportion of target to control splenocytes) was determined 18 h later by flow cytometry using a previously described method[31] (Figure 6c). Although the differences across particles are not considered statistically significant, the data clearly indicate reduced CTL activity in mice immunized with both M+C- and M+C+ particles. These results are further evidence supporting the hypothesis that NOD2 signaling inhibits CD8+ T cell responses.

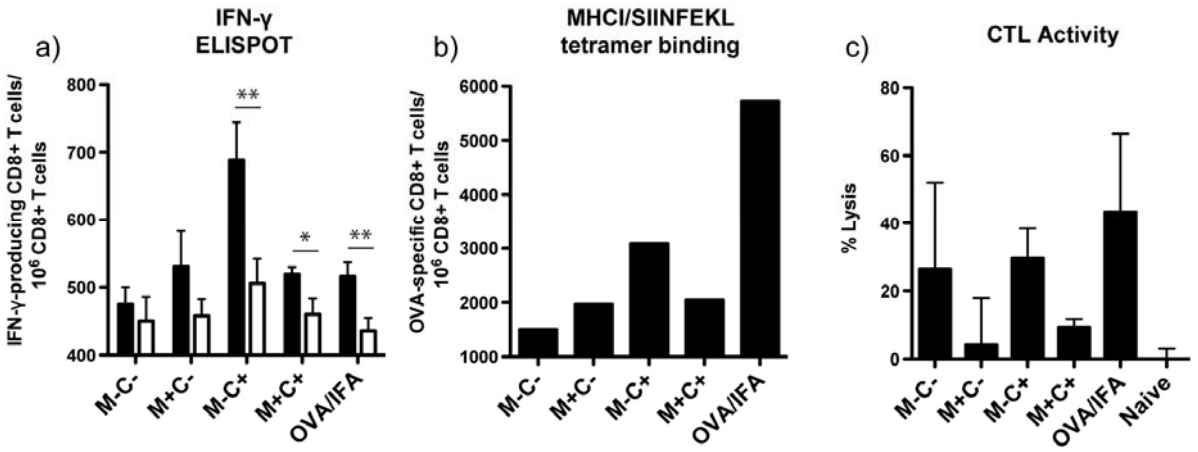

Figure 6. CD8+ T cell activation in vivo: a) The number of IFN-γ-producing CD8+ T cells per million CD8+ T cells when stimulated with splenocyte APCs and 2.5 μg OVA at 37 °C, 5% CO_2 ex vivo for 3 days measured using an ELISPOT assay (white bars represent cells incubated without OVA, and black bars cells incubated with OVA), b) Isolated CD8+ T cell population stained with a fluorescent tetramer of MHC class I molecules with loaded OVA epitopes (SIINFEKL) and quantified by flow cytometry, c) In vivo CTL assay, OVA-specific cell lysis (i.e., the change in the proportion of target (SIINFEKL pulsed) to control (unpulsed) splenocytes) determined by flow cytometry Data are expressed as the mean ± standard

deviation; *p < 0.05, **p < 0.01, ***p < 0.001; a: *t*-test. Each group in (a) and (b) shows data obtained from pooled cells of 5 individual mice. Each group in (c) shows data obtained from 3 individual mice.

CD4+ T cells are known to mediate CD8+ T cell activation through costimulation (i.e., "licensing") of dendritic cells (DCs), which influences the antigen presentation and costimulatory capacity necessary for activating primary CD8+ T cell responses.[32] The results suggest that the CD4+ T cell polarization that occurs due to NOD2/TLR9 signaling is associated with reduced CD8+ T cell activation. CD8+ T cell activation requires MHC class I presentation of particles, which were likely to be internalized by cells via endocytosis/phagocytosis. Several studies have demonstrated that TLR9 signaling with CpG can induce cross presentation of antigens in vitro and CD8+ T cell activation in vivo,[9,33] which is in agreement with the current studies. A recent study reported by Wagner et al. showed that NOD2 signaling inhibits cross presentation driven by LPS (TLR4 ligand),[34] which is also in agreement with the current results. While the mechanisms are not clear, it is evident that NOD2 activation alone is insufficient to induce a strong CTL response and has a negative effect on TLR9-driven CTL responses.

3. Conclusion

Reduced ovalbumin particles were rationally selected for functionalization with NOD2 and TLR9 agonists with the aim of enhancing immune responses through synergistic NOD and TLR signaling. NOD2 agonist, MDP, was conjugated to amines in OVA via amide bond formation and TLR9 agonist, CpG ODN, was covalently conjugated to free thiols in reduced OVA via thiol/disulfide exchange. The results showed that the combination of agonists induced synergistic inflammatory innate immune responses but had different effects on

adaptive immune responses in vivo. Specifically, NOD2 and TLR9 signaling induced Th2- and Th1-polarized CD4+ T cell and antibody responses, respectively, when delivered as single ligands. TLR9 signaling also induced CD8+ T cell responses. However, when the agonists were combined, enhanced Th1-polarized CD4+ T cell and antibody responses and decreased CD8+ T cell responses were observed.

The study demonstrates that NOD2 signaling can have different roles in modulating the adaptive immune response depending on the presence of TLR9 costimulation. In the absence of TLR9 signaling, NOD2 signaling leads to strongly polarized Th2 responses, which are also induced by current alum and emulsion adjuvants. However, in the presence of TLR9 costimulation, NOD2 signaling can significantly polarize away from Th2 and toward Th1 CD4+ T cell and antibody responses as well as suppress CD8+ T cell responses, whereas TLR9 signaling alone results in a Th1- and CD8+ T cell-mediated responses. A long-term goal in vaccinology is an understanding of how to rationally induce specific types of adaptive immune response, as the characteristics of desired adaptive immune responses vary across vaccine applications. The study shows that NOD2 signaling may be a promising strategy for enhancing TLR-driven Th1 CD4+ T cell and antibody responses while suppressing CD8+ T cell responses, which is valuable knowledge for rational adjuvant formulation.

4. Experimental Section

Materials. CpG (5'- TCC ATG ACG TTC CTG ACG TT -3'-thiol), GpC control (5'- TCC ATG AGC TTC CTG AGC TT -3'), and CpG-FITC custom ODNs were purchased from GeneWorks, Muramyl dipeptide (MDP) and MDP control ligands were purchased from InvivoGen. Poly(acrylic acid) (PAA), cetyltrimethylammonium bromide (CTAB), tetraethyl orthosilicate (TEOS), (3-aminopropyl)-triethoxysilane (APTES), albumin from chicken egg white (OVA), 2-(N-morpholino)ethanesulfonic acid hydrate (MES), 3-(N-

morpholino)propanesulfonic acid (MOPS), 4-(4,6-dimethoxy-1,3,5-triazin-2-yl)-4-methylmorpholinium chloride (DMTMM), dithiothreitol (DTT), dithionitrobenzoic acid (DTNB), hydrofluoric acid (HF), Red Blood Cell Lysing Buffer, Mytomycin-C, and Incomplete Freund's Adjuvant (IFA), goat anti-mouse, horseradish peroxidase swine anti-goat, and 2,2'-azino-bis(3-ethylbenzothiazoline-6-sulphonic acid) (ABTS) were purchased from Sigma-Aldrich and used as received. Dulbecco's Phosphate-Buffered Saline (DPBS) was obtained from Life Technologies. 3H-thymidine was purchased from GE Healthcare Life Sciences. Ultrapure water with resistance greater than 18 MΩ cm was obtained from an inline Millipore RiOs/Origin system (Millipore Corporation, USA) (Milli-Q, MQ).

Preparation and Amine-Functionalization of MS Templates. MS particles were synthesized according to a modified literature method.[35] Briefly, 1.1 g of CTAB was completely dissolved in 50 mL of water with stirring. Subsequently, 4.3 g of PAA solution was added with vigorous stirring at room temperature (25 °C) until a clear solution was obtained. Next, 3.5 mL of ammonium hydroxide solution was added to the above solution with vigorous stirring, resulting in a milky suspension. After stirring for 20 min, 4.46 mL of TEOS was added to the above solution. After further stirring for 15 min, the mixture was transferred into a 100 mL Teflon-sealed autoclave, which was left at 100 °C for 48 h. The as-synthesized MS particles were washed with Milli-Q water and ethanol three times, and finally dried at 80 °C overnight. The organic templates were removed by calcination at 550 °C for 6 h. 30 mg of the synthesized MS particles was dispersed in 900 mL of 70% (v/v) ethanol, followed by incubation with 50 μL of ammonia solution and 30 μL of APTES overnight. The modified particles were washed with ethanol and Milli-Q water three times.

Preparation of Reduced OVA Particles with Chemically Conjugated MDP and CpG. 2 mg mL^{-1} APTES-modified MS silica particles were dispersed in 2 mg mL^{-1} OVA solution in MES buffer (50 mM, pH 6). The particle dispersion was allowed to incubate for 4 h at 25 °C

with constant agitation to allow OVA infiltration via electrostatic surface adsorption. Following incubation, excess OVA was removed by centrifugation, and particles were washed with MES buffer (50 mM, pH 6). Loaded OVA was reduced by dispersing 100 mg mL^{-1} MS silica particles with loaded OVA in MOPS buffer (20 mM, pH 8) containing 0.5 M DTT and incubated for 30 min at 37 °C with constant agitation. Particles were washed with MES buffer (50 mM, pH 6) and 5 mg mL^{-1} MS particles were dispersed in MES buffer (50 mM, pH 6) containing 2 mg mL^{-1} MDP (or MDP control) (i.e., ~100:1 MDP to OVA mole ratio) and 10 mg mL^{-1} DMTMM and allowed to incubate overnight (~16 h) at 25 °C with constant agitation. Particles were washed with sodium phosphate buffer (100 mM, pH 8) and 5 mg mL^{-1} MS particles were dispersed in sodium phosphate buffer (100 mM, pH 8) containing 2 mg mL^{-1} DTNB and allowed to incubate for 5 h at 25 °C with constant agitation. Particles were washed with DPBS and 5 mg mL^{-1} MS particles were dispersed in DPBS containing 100 μg mL^{-1} CpG ODN (or GpC ODN control) and allowed to incubate overnight (~16 h) at 25 °C with constant agitation. MS templates were dissolved with 2M HF/8M NH_4F solution (pH ~5). *Caution! HF is highly toxic. Extreme care should be taken when handling HF solution, and only small quantities should be prepared.* The resulting OVA particles were washed with MQ.

NOD2 and TLR9 Activation in HEK293 Reporter Cell Lines. HEK-mNOD2, HEK-mTLR9, HEK-Null1, and HEK-Null2 cells were plated at a concentration of 40^4 cells in 200 μL of DMEM containing 10% HI FBS, 2 mM L-glutamine in a V-bottom 96-well plate. 10^7 particles were added to the cells and allowed to incubate for 24 h at 37 °C, 5% CO_2. 50 μL of supernatant was taken from the cultures and 150 μL QUANTI-Blue was added and allowed to incubate for 2 h. Optical density was measured at 620 nm to quantify SEAP levels.

NK-kB Activation in RAW-Blue Reporter Cell Line. RAW-Blue cells were plated at a concentration of 10^5 cells in 200 μL of DMEM containing 10% HI FBS, 2 mM L-glutamine

in a V-bottom 96-well plate. 10^7 particles were added to the cells and allowed to incubate for 24 h at 37 °C, 5% CO_2. 50 μL of supernatant was taken from the cultures and 150 μL QUANTI-Blue was added and allowed to incubate for 2 h. Optical density was measured at 620 nm to quantify SEAP levels.

Cytokine and Chemokine Bio-Plex Assay with RAW Cells. RAW cells were plated at a concentration of 10^5 cells in 200 μL of DMEM containing 10% HI FBS, 2 mM L-glutamine in a V-bottom 96-well plate. 10^7 particles were added to the cells and allowed to incubate for 24 h at 37 °C, 5% CO_2. Supernatant was removed and spun at 8000 rcf to remove particulate matter before being stored at -30 °C. Cytokine levels in the supernatants were measured using a Bio-Plex Pro Mouse Cytokine Standard 8-Plex, Group 1 kit according to the manufacturer's instructions.

Mice. C57BL/6 mice were obtained from the Walter and Eliza Hall Institute (WEHI) animal facility and were housed in specific pathogen-free conditions at the Biological Research Facility in the Royal Dental Hospital of Melbourne. Animal experimentation was approved by the University of Melbourne Animal Ethics Committee.

Immunization. Groups of five female C57/Bl6 mice 6-8 weeks old were immunized intraperitoneally with 25 μL of either 1 mg mL^{-1} OVA particles or a 1:1 water-in-oil emulsion of 1 mg mL^{-1} OVA protein in DPBS and IFA. After 21 days the mice were given a booster subcutaneously injection with the same antigens. Then 21 days after the booster injection, mice were bled and spleens were taken for antibody ELISAs and T cell assays, respectively. For the CD8/CTL assays mice were immunized (day 0) intraperitoneally with 25 μL of either 1 mg mL^{-1} OVA particles or a 1:1 water-in-oil emulsion of 1 mg mL^{-1} OVA protein in DPBS and IFA and used in the in vivo CTL assay described below.

CD4+ T cell Proliferation. Particles or free OVA were added to 96-well flat-bottom cell culture plates. Suspensions of 3 x 10^5 APCs and 3 x 10^5 T cells were cultured onto the plates.

3H-thymidine was added after ~70 h of incubation at 37 °C, 5% CO_2. 3H-thymidine incorporation was assessed using a beta counter 24 h later (i.e., ~94 h incubation total).

Cytokine Bio-Plex Assay with CD4+ T cells. Particles or free OVA was added to 96-well flat-bottom cell culture plates. Suspensions of 3 x 10^5 APCs and 3 x 10^5 T cells were cultured onto the plates and allowed to incubate for 72 h at 37 °C, 5% CO_2. Cytokine levels in the supernatants were measured using a Bio-Plex Pro Mouse Cytokine Standard 8-Plex, Group 1 kit according to the manufacturer's instructions.

ELISPOT Assays. 2.5 μg of either OVA particles or free OVA was added to 96-well IL-4 and IFN-γ ELISPOT plates (Millipore). Suspensions of 3 x 10^5 APCs and 3 x 10^5 T cells were cultured onto the plates and ELISPOT plates were developed after ~70 h of incubation at 37 °C, 5% CO_2.

CD8+ T cell Quantification by Flow Cytometry. CD8+ T cells from five individual mice were pooled per immunization group and CD8+ T cells isolated using CD8-microbeads and autoMACS separation. Cells were incubated with a fluorescent MHC class I OVA-specific tetramer (SIINFEKL/H2Kb) conjugated to PE (obtained from the Brookes laboratory, The University of Melbourne), anti-mouse CD8 monoclonal antibody conjugated to APC (BD Biosciences, clone 53-6.7), and mouse Fc Block™ (BD Biosciences, cat# 553141) for 20 min on ice. Cells were washed with DPBS and analyzed by flow cytometry using a Beckman Coulter FC 500 flow cytometer.

In Vivo CTL Assay. In vivo cytotoxic T cell activity was determined using the method described by Mueller et al.[31] Target and control splenocyte cells were prepared from donor naïve mice. Target splenocytes were pulsed/incubated in media without FBS (1 hour, 37 °C) with 1 μg/mL SIINFEKL peptide (OVA 257-264), washed (800 *g*, 5 min), and then labeled with a high concentration (1.0 μM, 20 min, 37 °C) of CFSE (CFSEhigh population); or control splenocytes incubated without peptide and labeled with a low concentration (0.1 μM,

20 min, 37 °C) of CFSE (CFSElow population). Equal number of cells from each population were mixed together and 10^7 cells of each population (2×10^7 cells/200μL in PBS) was adoptively transferred into recipient (immunized, see above) mice via tail vein injection six days after the immunization. The recipient mice were then killed 18 hours later and the spleens isolated and single cell suspension made from each recipient and analyzed by flow cytometry using a Beckman Coulter FC 500 flow cytometer. Each population was distinguished by their different fluorescent intensities. Lysis was determined by loss of the peptide-pulsed CFSEhigh population from the splenocytes in relation to the peptide-negative CFSElow population.

Serum IgG ELISA Assay. C57/Bl6 mice 6-8 weeks old were immunized intraperitoneally with 25 μL of either 1 mg mL^{-1} OVA particles or a 1:1 water-in-oil emulsion of 1 mg mL^{-1} OVA protein in DPBS and IFA. After 21 days the mice were given a booster subcutaneously injection with the same antigens and then bled 10 days later. The collected sera were individually stored at -20 °C. ELISAs were performed on sera from five mice in each group. 10 μg mL^{-1} OVA protein in DPBS was used to coat wells of 96-well flat-bottom polystyrene EIA/RIA plate (Corning Costar) plates overnight at 4 °C. The coating solution was removed and 5% (wt/vol) skim milk powder in PBS was added to block the remaining uncoated surface for 1 h at room temperature. Wells were then washed three times with PBS-T (0.01% Tween-20) and once with PBS. Double dilutions of subject sera in PBS containing 2.5% (wt/vol) skim milk powder from 1/12.5 to 1/1600 were added to wells and incubated overnight at 4 °C. Wells were washed three times with PBS-T and once with PBS and incubated with goat anti-mouse (2.5% skim milk/PBS) directed against total IgG (1/4000 dilution) for 1 h at room temperature. Wells were washed three times with PBS-T and once with PBS and bound antibody was detected by incubation with horseradish peroxidase-conjugated swine anti-goat (1/4000 dilution) for 1 h at room temperature. Wells were washed

three times with PBS-T and once with PBS. Substrate, ABTS in 50 mM citric acid buffer containing 0.02% (vol/vol) hydrogen peroxide was added. After incubation for approximately 1 h, optical density at 405 nm was measured using a microplate reader.

Supporting Information
Supporting Information is available from the Wiley Online Library or from the author.

Acknowledgements

This work was supported by the Australian Research Council (ARC) under the Australian Laureate Fellowship (F.C., FL120100030), Discovery Early Career Researcher Award (Y.Y., DE130100488), and ARC Centre of Excellence in Convergent Bio-Nano Science and Technology (CE140100036) schemes, as well as a National Health and Medical Research Council Project Grant (APP1029878). K.T.G. acknowledges funding from the Australian Government through an International Postgraduate Research Scholarship and an Australian Postgraduate Award.

Received: ((will be filled in by the editorial staff))
Revised: ((will be filled in by the editorial staff))
Published online: ((will be filled in by the editorial staff))

[1] E. Bergmann-Leitner, W. Leitner, *Vaccines* **2014**, *2*, 252.

[2] R. Seder, S. G. Reed, D. O'Hagan, P. Malyala, U. D'Oro, D. Laera, S. Abrignani, V. Cerundolo, L. Steinman, S. Bertholet, *Vaccine* **2015**, *33*, B40.

[3] K. Timmermans, T. S. Plantinga, M. Kox, M. Vaneker, G. J. Scheffer, G. J. Adema, L. A. B. Joosten, M. G. Netea, *Clin. Vaccine Immunol.* **2013**, *20*, 427.

[4] N. W. Palm, R. Medzhitov, *Immunol. Rev.* **2009**, *227*, 221.

[5] A. Iwasaki, R. Medzhitov, *Nat. Immunol.* **2015**, *16*, 343.

[6] a) F. Steinhagen, T. Kinjo, C. Bode, D. M. Klinman, *Vaccine* **2011**, *29*, 3341; b) M. S. Duthie, H. P. Windish, C. B. Fox, S. G. Reed, *Immunol. Rev.*. **2011**, *239*, 178.

[7] K. Geddes, J. G. Magalhaes, S. E. Girardin, *Nat. Rev. Drug Discov.* **2009**, *8*, 465.

[8] a) A. Iwasaki, R. Medzhitov, *Nat. Immunol.* **2004**, *5*, 987; b) M. Schnare, G. M. Barton, A. C. Holt, K. Takeda, S. Akira, R. Medzhitov, *Nat. Immunol.* **2001**, *2*, 947; c) C. Pasare, R. Medzhitov, *Immunity* **2004**, *21*, 733; d) A. L. Gavin, K. Hoebe, B. Duong, T. Ota, C. Martin, B. Beutler, D. Nemazee, *Science* **2006**, *314*, 1936.

[9] a) S. K. Datta, V. Redecke, K. R. Prilliman, K. Takabayashi, M. Corr, T. Tallant, J. DiDonato, R. Dziarski, S. Akira, S. P. Schoenberger, E. Raz, *J. Immunol.* **2003**, *170*, 4102; b) S. K. Datta, E. Raz, *Springer Semin. Immunopathol.* **2005**, *26*, 247.

[10] a) I. Jelinek, J. N. Leonard, G. E. Price, K. N. Brown, A. Meyer-Manlapat, P. K. Goldsmith, Y. Wang, D. Venzon, S. L. Epstein, D. M. Segal, *J. Immunol.* **2011**, *186*, 2422; b) O. Schulz, S. S. Diebold, M. Chen, T. I. Naslund, M. A. Nolte, L. Alexopoulou, Y. T. Azuma, R. A. Flavell, P. Liljestrom, C. R. E. Sousa, *Nature* **2005**, *433*, 887; c) T. Maurer, A. Heit, H. Hochrein, F. Ampenberger, M. O'Keeffe, S. Bauer, G. B. Lipford, R. M. Vabulas, H. Wagner, *Eur. J. Immunol.* **2002**, *32*, 2356; d) K. Schwarz, T. Storni, V. Manolova, A. Didierlaurent, J. C. Sirard, P. Rothlisberger, M. F. Bachmann, *Eur. J. Immunol.* **2003**, *33*, 1465; e) J. Z. Oh, J. S. Kurche, M. A. Burchill, R. M. Kedl, *Blood* **2011**, *118*, 3028.

[11] a) J. H. Fritz, L. Le Bourhis, G. Sellge, J. G. Magalhaes, H. Fsihi, T. A. Kufer, C. Collins, J. Viala, R. L. Ferrero, S. E. Girardin, D. J. Philpott, *Immunity* **2007**, *26*, 445; b) J. G. Magalhaes, J. H. Fritz, L. Le Bourhis, G. Sellge, L. H. Travassos, T. Selvanantham, S. E. Girardin, J. L. Gommerman, D. J. Philpott, *J. Immunol.* **2008**, *181*, 7925.

[12] a) J. H. Fritz, S. E. Girardin, C. Fitting, C. Werts, D. Mengin-Lecreulx, M. Caroff, J. M. Cavaillon, D. J. Philpott, M. Adib-Conquy, *Eur. J. Immunol.* **2005**, *35*, 2459; b) H. Tada,

S. Aiba, K. I. Shibata, T. Ohteki, H. Takada, *Infect. Immun.* **2005**, *73*, 7967; c) H. Takada, A. Uehara, *Curr. Pharm. Des.* **2006**, *12*, 4163.

[13] V. Pavot, N. Rochereau, J. Resseguier, A. Gutjahr, C. Genin, G. Tiraby, E. Perouzel, T. Lioux, F. Vernejoul, B. Verrier, S. Paul, *J. Immunol.* **2014**, *193*, 5781.

[14] M. Skwarczynski, I. Toth, *Nanomedicine* **2014**, *9*, 2657; C. Foged, *Ther. Delivery* **2011**, *2*, 1057.

[15] a) J. W. Cui, R. De Rose, J. P. Best, A. P. R. Johnston, S. Alcantara, K. Liang, G. K. Such, S. J. Kent, F. Caruso, *Adv. Mater.* **2013**, *25*, 3468; b) S. De Koker, J. W. Cui, N. Vanparijs, L. Albertazzi, J. Grooten, F. Caruso, B. G. De Geest, *Angew. Chem.* **2016**, *128*, 1356; *Angew. Chem. Int. Ed.* **2016**, *55*, 1334.

[16] K. T. Gause, Y. Yan, J. Cui, N. M. O'Brien-Simpson, J. C. Lenzo, E. C. Reynolds, F. Caruso, *ACS Nano* **2015**, *9*, 2433.

[17] N. Inohara, Y. Ogura, A. Fontalba, O. Gutierrez, F. Pons, J. Crespo, K. Fukase, S. Inamura, S. Kusumoto, M. Hashimoto, S. J. Foster, A. P. Moran, J. L. Fernandez-Luna, G. Nunez, *J. Biol. Chem.* **2003**, *278*, 5509.

[18] F. Martinon, L. Agostini, E. Meylan, J. Tschopp, *Curr. Biol.* **2004**, *14*, 1929.

[19] C. Wischke, S. Mathew, T. Roch, M. Frentsch, A. Lendlein, *J. Controlled Release* **2012**, *164*, 299.

[20] V. Pavot, N. Rochereau, C. Primard, C. Genin, E. Perouzel, T. Lioux, S. Paul, B. Verrier, *J. Controlled Release* **2013**, *167*, 60.

[21] P. Malyala, D. T. O'Hagan, M. Singh, *Adv. Drug Deliv. Rev.* **2009**, *61*, 218.

[22] C. Werts, S. E. Girardin, D. J. Philpott, *Cell Death Differ.* **2006**, *13*, 798.

[23] M. S. Lee, Y. J. Min, in *Annu. Rev. Biochem.*, Vol. 76, **2007**, pp. 447-480.

[24] S. H. Yang, R. Tamai, S. Akashi, O. Takeuchi, S. Akira, S. Sugawara, H. Takada, *Infect. Immun.* **2001**, *69*, 2045.

[25] a) C. M. Chen, Y. S. Gong, M. Zhang, J. J. Chen, *J. Biol. Chem.* **2004**, *279*, 25876; b) M. Hasegawa, Y. Fujimoto, P. C. Lucas, H. Nakano, K. Fukase, G. Nunez, N. Inohara, *EMBO J.* **2008**, *27*, 373.

[26] P. Pelegrin, C. Barroso-Gutierrez, A. Surprenant, *J. Immunol.* **2008**, *180*, 7147.

[27] D. Ferrari, C. Pizzirani, E. Adinolfi, R. M. Lemoli, A. Curti, M. Idzko, E. Panther, F. Di Virgilio, *J. Immunol.* **2006**, *176*, 3877.

[28] C. Pasare, R. Medzhitov, *Nature* **2005**, *438*, 364; C. R. Ruprecht, A. Lanzavecchia, *Eur. J. Immunol.* **2006**, *36*, 810.

[29] T. Petterson, J. Jendholm, A. Mansson, A. Bjartell, K. Riesbeck, L. O. Cardell, *J. Leukoc. Biol.* **2011**, *89*, 177.

[30] a) L. Lin, A. J. Gerth, S. L. Peng, *Eur. J. Immunol.* **2004**, *34*, 1483; b) N. S. Liu, N. Ohnishi, L. Ni, S. Z. Akira, K. B. Bacon, *Nat. Immunol.* **2003**, *4*, 687.

[31] S. N. Mueller, C. M. Jones, A. T. Stock, M. Suter, W. R. Heath, F. R. Carbone, *J. Immunol.* **2006**, *176*, 7379.

[32] B. J. Laidlaw, J. E. Craft, S. M. Kaech, Nat. Rev. Immunol. 2016, 16, 102.

[33] R. Mandraju, S. Murray, J. Forman, C. Pasare, *J. Immunol.* **2014**, *192*, 4303.

[34] C. S. Wagner, P. Cresswell, *J. Immunol.* **2012**, *188*, 686.

[35] J.G. Wang, H.J. Zhou, P.-C. Sun, D.T. Ding, T.H. Chen, *Chem. Mater.* **2010**, *22*, 3829.

Table of Contents entry

Codelivery of NOD2 and TLR9 agonists via covalent attachment to mesoporous silica-templated protein antigen particles results in synergistic innate immune responses in vitro and adaptive immune responses in mice that are both quantitatively and qualitatively different than those induced by particles containing either NOD2 or TLR9 agonists alone.

Keywords: adjuvant, vaccine, protein particles, codelivery, mesoporous silica

K. T. Gause, Y. Yan, N. M. O'Brien-Simpson, J. Cui, J. C. Lenzo, E. C. Reynolds, F. Caruso*

Codelivery of NOD2 and TLR9 Ligands via Nanoengineered Protein Antigen Particles for Improving and Tuning Immune Responses

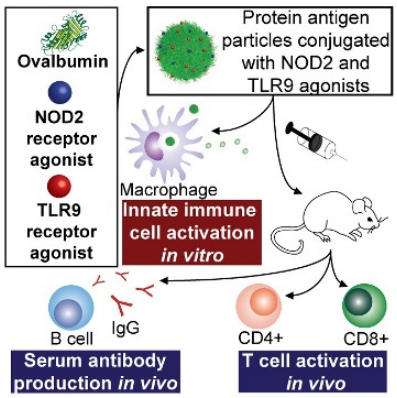

Author/s:
Gause, KT; Yan, Y; O'Brien-Simpson, NM; Cui, J; Lenzo, JC; Reynolds, EC; Caruso, F

Title:
Codelivery of NOD2 and TLR9 Ligands via Nanoengineered Protein Antigen Particles for Improving and Tuning Immune Responses

Date:
2016-11-02

Citation:
Gause, K. T., Yan, Y., O'Brien-Simpson, N. M., Cui, J., Lenzo, J. C., Reynolds, E. C. & Caruso, F. (2016). Codelivery of NOD2 and TLR9 Ligands via Nanoengineered Protein Antigen Particles for Improving and Tuning Immune Responses. ADVANCED FUNCTIONAL MATERIALS, 26 (41), pp.7526-7536. https://doi.org/10.1002/adfm.201603563.